# Long-Wavelength PtSi Infrared Detectors Fabricated by Incorporating a $P^+$ Doping Spike Grown by Molecular Beam Epitaxy

T. L. Lin, J. Park, T. George, E. W. Jones, R. W. Fathauer, and J. Maserjian

Center for Space Microelectronics Technology
Jet Propulsion Laboratory, California Institute of Technology
Pasadena, CA 91109

# ABSTRACT

By incorporating a 1-rim-thick p+ doping spike at the PtSi/Si interface, we have successfully demonstrated extended cutoff wavelengths of PtSi Schottky infrared detectors in the long wavelength infrared (LWIR) regime for the first time. The extended cutoff wavelengths resulted from the combined effects of an increased electric field near the silicide/Si interface due to the p+ doping spike and the Schottky image force. The p+ doping spikes were grown by molecular beam epitaxy at 450 ‘C using elemental boron as the dopant source, with doping concentrations ranging from 5 x $10^{19}$ to 2 x $10^{20}$ $cm^{-3}$. Transmission electron microscopy indicated good crystalline quality of the doping spikes. The cutoff wavelengths were shown to increase with increasing doping concentrations of the p+ spikes. Thermionic emission dark current characteristics were observed and photoresponse in the LWIR regime was demonstrated.

Silicide Schottky-barrier detectors are among the most promising infrared sensors for large focal plane array applications due to their advantages of uniformity, reliability, and low cost. State-of-the-art silicide PtSi focal plane arrays are used for imaging in the 3-5 μm medium wavelength infrared (MWIR) region. 640 x 480 and 1024 x 1024 element PtSi imaging arrays have been demonstrated".

The PtSi spectral response follows the Fowler dependence, and its quantum efficiency (QE) is given by

$$QE = C_1 \frac{(h\nu - q\phi_B)^2}{h\nu} = 1.24\, C_1\, \lambda \left(\frac{1}{\lambda} - \frac{1}{\lambda_c}\right)^2 \tag{1}$$

where $C_1$ is the emission coefficient, $h\nu$ and $\lambda$ are the energy and the wavelength of the incident photon, respectively, $q\phi_B$ is the Schottky barrier height, and $\lambda_c$ is the cutoff wavelength, given by

$$\lambda_c = \frac{1.24}{q\phi_B}. \tag{2}$$

The Schottky barrier height of the PtSi detector is -0.22 eV, corresponding to a cutoff wavelength of -5.6 μm. Due to the Fowler dependence, the QE of the PtSi detector in the 3-5 μm MWIR regime is relatively low.

There is a great interest in extending the PtSi cutoff wavelength for long wavelength infrared (LWIR) operation in the 8-14 μm regime and for improved MWIR performance. The Schottky barrier height is determined by the combined effects of the image-force effect and the electric field of the depletion region. Consequently, the effective PtSi Schottky barrier height can be reduced by introducing a thin p-type doped layer at the silicide/Si interfaces. Due to the enhanced electric field of the doping spike, a potential spike near the PtSi/Si interface was formed, allowing photo-excited holes to tunnel into the substrate, resulting in a lower effective potential barrier. Previously, very shallow ion implants at the metal-silicon interface, first demonstrated by Shannon[6], have been employed by Pellegrini *et al.* and Wei *et al.* to extend the PtSi cutoff wavelength[7,8]. More recently, molecular beam epitaxy (MBE) was used to grow the thin doping spikes to reduce the Schottky barriers of Ti/Si[9] and $CoSi_2$/Si[10]. However, the additional tunneling process required for the collection of the photo-excited carriers reduces the detector response. Furthermore, due to the limited abruptness of the implanted doping spike profile, the electric field near the doping spike was increased drastically, resulting in a significantly increased contribution of tunneling current to the detector dark current.

By reducing the doping spike thickness, the effective potential barrier can be reduced without the formation of a potential spike, eliminating the undesired tunneling process. The calculated energy-band diagrams of three PtSi detectors are shown in Fig. 1: (a) without the doping spike, (b) with a 5-rim-thick doping spike doped with 6 x $10^{18}$ $cm^{-3}$ boron, and (3) with a l-rim-thick doping spike doped with 1.2 x $10^{20}$ $cm^{-3}$ boron. The substrate doping concentration is 5 x $10^{14}$ $cm^{-3}$, and the bias voltage is -1 V for the calculation. The effective Schottky barrier heights for both doping-spike PtSi detectors are designed to be 0.1 eV. As shown in Fig. 1 (b), the thicker doping spike (5 nm) results in the formation of a potential spike, and the tunneling process will be required for the collection of photo-excited holes. By reducing the doping spike thickness to 1 nm, with a corresponding increase of the doping concentration from 6 x $10^{18}$ to 1.2 x $10^{20}$ $cm^{-3}$, similar barrier reduction can be achieved without the formation of an undesired potential spike, as shown in Fig. 1 (c), eliminating the undesirable tunneling process.

This thin doping spike approach requires the formation of - l-rim-thick doping spikes with high doping concentrations and atomically abrupt doping profiles. This was made possible by the recent advances in the MBE technology, which allows the growth of degenerately doped silicon iayers with atomically sharp doping profiles at a low temperature [1,12]. The low growth temperature is essential to preserve the atomically sharp doping profiles to avoid the boron precipitation and surface segregation problems[11]. In this paper, we report extended LWIR cutoff wavelengths of PtSi Schottky infrared detectors by incorporating 1-rim-thick p+ doping spikes grown by MBE.

The PtSi Schottky detectors were fabricated on double-side polished Si (1 00) wafers with a resistivity of 30 Q-cm. The device structure incorporates n-type guard rings which define the periphery of the active device areas to suppress edge leakage. Prior to MBE growth, the wafers were cleaned using the “spin-clean” method, which involves the removal of a chemically grown surface oxide using an HF/ethanol solution in a nitrogen glove box followed by annealing in the growth chamber of a commercial Riber EVA 32 Si MBE system at temperatures less than 500°C[13]. The 1 -rim-thick $p^+$-Si iayers were grown by MBE at 450 “C using elemental boron as the dopant source. Doping concentrations ranging from 5 xl $0^{19}$ to 2 x $10^{20}$ $cm^{-3}$ were studied. The PtSi iayers were formed in-situ by depositing undoped Si and Pt followed by annealing at 400°C. The PtSi infrared detectors were characterized using current-voltage (i-V) measurements and photo response measurements. The material quality of the p-t doping spikes and the. PtSi layers were characterized by cross-sectional transmission electron microscopy (TEM) using an ABT 002B 200 kV high resolution electron microscope. Cross-sectional TEM specimens were prepared using standard mechanical dimpling followed by Ar ion thinning.

Figure 2 shows the cross-sectional TEM micrograph of the PtSi/Si interface of detector A. The thickness and the doping concentration of the $p^+$ spike are 1 nm and 5 x $10^{19}$ $cm^{-3}$, respectively, and the thickness of the PtSi layer is 2.4 nm. The PtSi layer has a **uniform thickness** and a reasonably flat interface with the underlying Si as indicated by the single arrow in Fig. 2. It is polycrystalline in nature with some grains exhibiting lattice fringes and moire-fringe patterns. No evidence was found for structural damage in the crystal due to the presence of this layer.

The dark currents of the doping-spike PtSi detectors were thermionic emission limited, given by Jo = A*" $T^2 \exp(-q\phi_B/kT)$, where $J_o$ is the dark current density, A** is the Richardson constant, T is the absolute temperature, $q\phi_B$ is the effective potential barrier, and k is the Boltzmann constant. Figure 3 shows the typical plot of $J_o/T^2$ vs 1/kT for a doping-spike PtSi detector measured at -0.5 V reverse bias. The doping concentration of the l-rim-thick p+ doping spike is 2 x $10^{20}$ $cm^{-3}$. The cutoff wavelength of this detector determined by the Fowler plot is 22 µm, corresponding to a optical barrier height of 0.057 eV, as shown in Fig. 4. An effective barrier height, $q\phi_B$, of 0.032 eV was determined from the slope of the plot. The **0.025** eV **discrepancy** between the measured electrical and optical barrier heights is probably due to the scattering required for the internal photoemission process [14]. No excess tunneling dark current was observed, indicating the absence of tunneling effect.

The detector spectral responses were measured with back-side illumination using a 940K blackbody source. Figure **4 shows** the responses of three doping-spike PtSi detectors at T = 30K. The thickness of the PtSi layers is **4** nm and the doping concentrations of the 1-rim-thick doping spikes ranging from 1 x $10^{20}$ $cm^{-3}$ to 2 x $10^{20}$ $cm^{-3}$. The effective optical potential barriers of these detectors were determined by Fowler plots to be **0.09, 0.069,** and 0.057 eV, corresponding to cutoff wavelengths of 14, 18, and 22 µm, respectively, with the Fowler coefficients $C_1$'s of 0.2, 0.156, and '0.1 43 $eV^{-1}$, respectively. A higher $C_1$ of 0.2 was observed for the 14 µm cutoff detector because an optical cavity was incorporated to enhance the infrared absorption. These Cl's were comparable to those of conventional PtSi detectors with similar PtSi thicknesses, indicating the absence of the tunneling process in the internal photoemission process.

In conclusion, the cutoff wavelength of the PtSi Schottky infrared detector has been extended to the LWIR region by incorporating a 1 -rim-thick $p^+$ doping spike at the silicide/silicon interface. The detector cutoff wavelengths can be tailored by varying the doping concentrations of the $p^+$ spikes. Cutoff wavelengths of 14, 18, and 22 µm have been demonstrated for doping-spike PtSi detectors. Thermionic emission I-V characteristics and Fowler-dependent photo responses were observed for the doping-spike PtSi detectors, indicating the absence of undesirable tunneling 'mechanism.

We **would like to thank** F. D. **Shepherd for helpful** discussions, The **work** described in this paper was performed by the Center for Space Microelectronics Technology, Jet Propulsion Laboratory, California Institute of Technology and was jointly sponsored by the National Aeronautics and Space Administration, Office of Aeronautics, Exploration and Technology and the Strategic Defense Initiative Organization, Innovative Science and Technology Office.

REFERENCES

1. D. J. Sauer, F. V. Shallcross, F. L. Hsueh, G. M. Meray, P. A, Levine, H. R. Gilmartin, T. S, Villani, B. J. Esposito, and J. R. Tower, Proc. SPIE, Vol. 1540, *Infrared Technology XVII*, edited by Spiro, Anderson, andScholl, pp. 285-296, 1991.
2. J. L. Gates, W. G, Connelly, T. D. Franklin, R. E. Mills, F. W. Price, and T. Y. Wittwer, Proc. SPIE, Vol. 1540, *Infrared Technology XVII*, edited by Spiro, Anderson andScholl, pp. 297-302, 1991.
3. D. L. Clark, J. R. Berry, G. L. Compagna, M. A, Cosgrove, G. G. Furman, J. R, Heydweiller, H. Honickman, R. A. Rehberg, P. H. Solie, and E. T. Nelson, Proc. SPIE, Vol. 1540, *Infrared Technology XV//,* edited by Spiro, Anderson and **Scholl,** pp. 303-311, 1991.
4. M. Kimata, N. Yutani, and S. N. Tsubouchi, Proc. SPIE. Vol. 1762, *Infrared Technology XV///,* edited by Andersen and Shepererd, 1992 (to be published).
5. *S.* M. Sze, *Physics of Semiconductor Devices* (Wiley, New York, 1981 ), Chap. 5.
6. J. M. Shannon, Appl. Phys. Lett., 24, 369 (1974).
7. P. Pellegrini, M. Week, and C. E. Ludington, Proc. SPIE, Vol. 311, *Mosaic focal Plane Methodologies II*, edited by Chan and Hall, pp. 24-29, 1981.
8. C-Y. Wei, W. Tantraporn, W Katz, and G. Smith, Thin Solid Films, 93. 407, 1982.
9. W. C. Ballamy and Y. Ota, Appl. Phys, Lett., 39, 629 (1 981).
10. R. W. Fathauer, T. L. Lin, P. J. Grunthaner, J. Maserjian, and P. O. Andersson, Proc. SPIE, Voi. 877, *Innovative Science and Technology,* edited by C. Kukkonen, pp. 2-7, 1988.
11. C. P. Parry, S. M. Newstead. R. D. Barlow, P. Augustus, R. A. A. Kubiak, M.G. Dowsett, T. E. Whall, and E. H. c. Parker, Appt. Phys. Lett., 58, 181 (1 991).
12. T. L. Lin, T. George, E. W. Jones, and A. Ksendzov, Appl. Phys. Lett., 60, 380 (1 992).

13. P. J. Grunthaner, F. J. Grunthaner, R. W. Fathauer, T. L. Lin, F. D. Schowengerdt, M. H. Hecht, D. Bell, W. Kaiser, and J. I-i. Mazur, Thin Solid Films, 183, 1,97 (1989).

14. F. D. Shepherd, Proc. SPIE, Vol. 1735, *Infrared Detectors: State of the Art, 1992* (to be published).

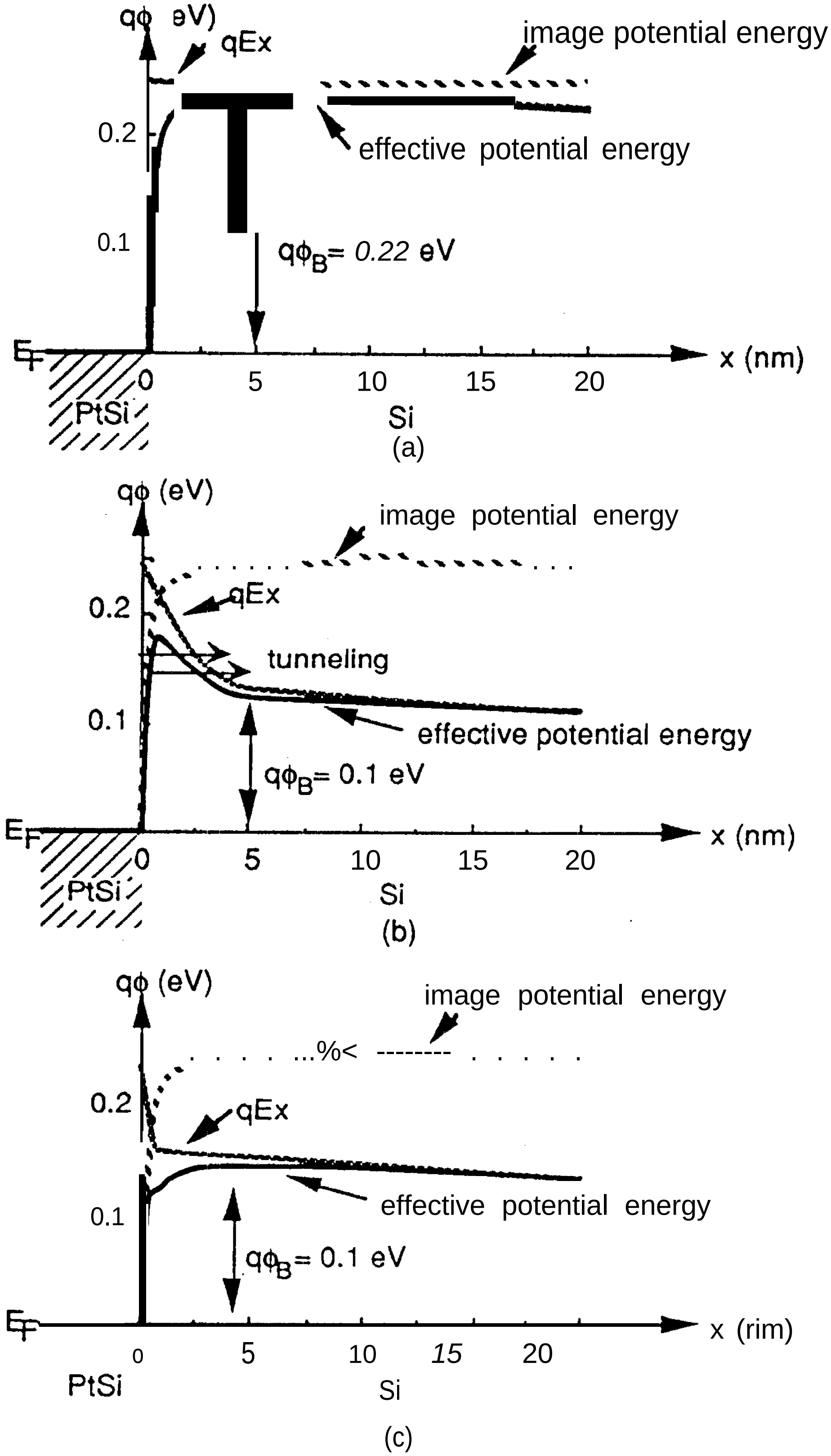


Figure 1. The calculated energy-band diagrams of three PtSi detectors incorporating the Schottky image force effect: (a) without the doping spike, (b) with a 5-rim-thick spike doped with 6 x $10^{18}$ $cm^{-3}$ boron, and (3) with a 1 -rim-thick spike doped with 1.2 x $10^{20}$ $cm^{-3}$ boron.

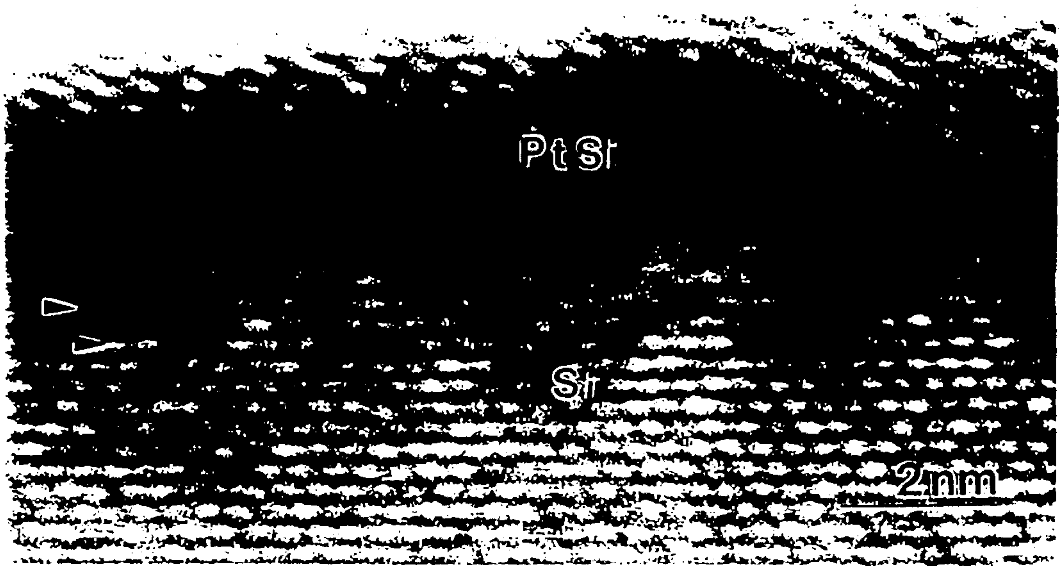


Figure 2. Cross-sectional TEM micrographs of a doping-spike PtSi detector with a 2.4-nm-thick PtSi layer and I-rim-thick p+ doping spike grown by ME3E at 450° C.

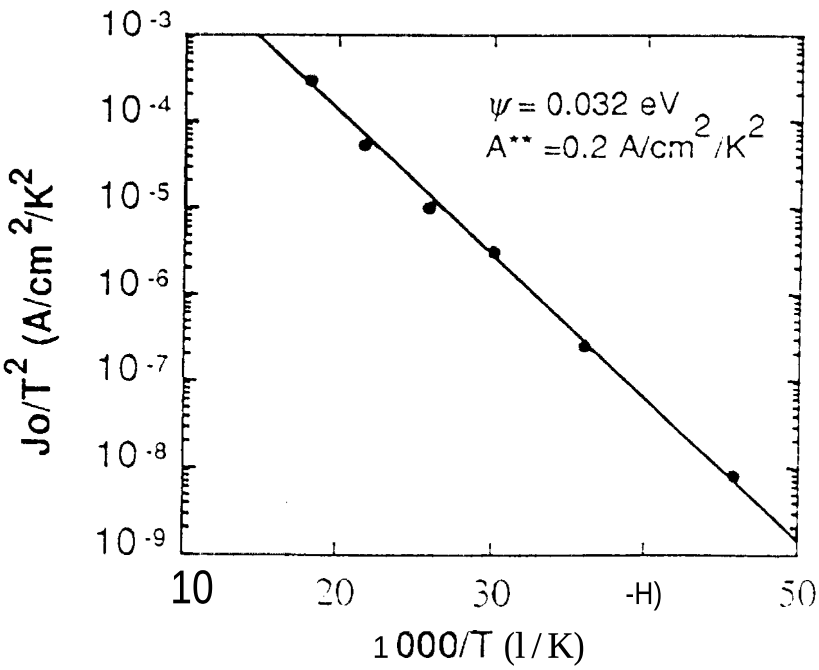


Figure 3. Richardson plot of a typical doping-spike PtSi detector with a 22 µm cutoff wavelength whose photo response is shown in Fig. 4.

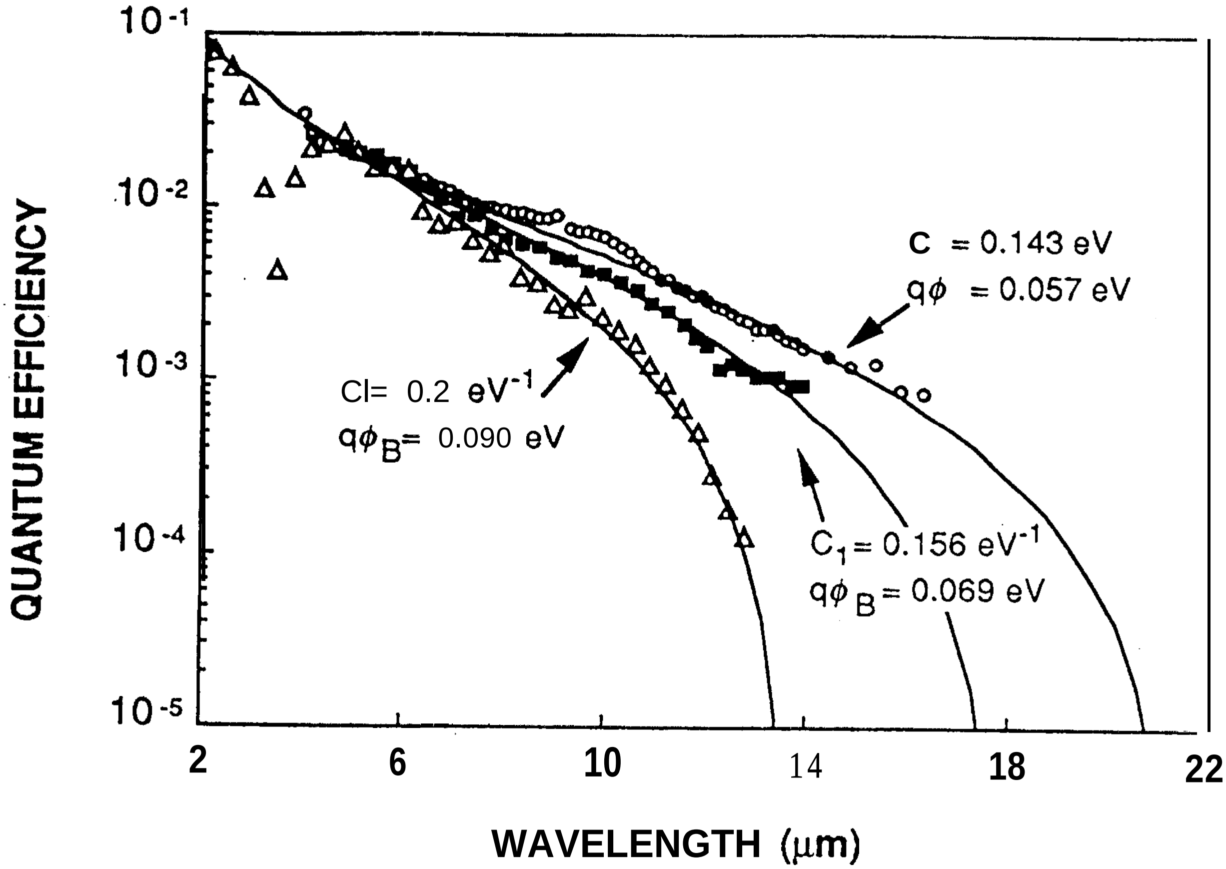


**Figure** 5. Quantum efficiency as a function of wavelength **for the three doping-spike** PtSi detectors with 1-rim-thick $p^+$ doping spikes measured at 40K. **The cutoff** wavelengths can be tailorable from 14 to 22 μm by increasing the p+ spike doping concentration from $1 \times 10^{20}$ to $2 \times 10^{20}\ cm^{-3}$.